Quantum chemical computations of Raman intensities: An ambiguity of the Placzek approximation

Jaroslav Šebestík and Petr Bouř*

Institute of Organic Chemistry and Biochemistry, Academy of Sciences, Flemingovo náměstí 2, 16610 Prague, Czech Republic

(Received 13 November 2024; revised 25 April 2025; accepted 28 April 2025; published 4 June 2025)

Coupled-perturbed (CP) computational methods, in particular those based on the density functional theory (DFT), are indispensable in interpretations of Raman scattering on molecules. The simulations are most often based on the Placzek approximation, ignoring the dependence of energies of the excited electronic states on nuclear coordinates. Thus practical CP DFT computations do not exactly correspond to the more general sum over state (SOS) formalism. We discuss this problem, investigate the SOS convergence, and formulate a distributed origin gauge enabling us to calculate origin-independent Raman optical activity intensities. The variations of the computed spectra caused by the energy gradient terms are investigated with practical examples. The results show that although the contribution of the gradient parts to Raman intensities is rather small in the far from resonance cases, their subtraction may still occasionally improve the simulated spectra. However, the effect is much more important for Raman optical activity and in resonance conditions. The possibility to correct the computed intensities for the gradient contribution thus opens a way for systematic improvements of quantum-mechanical simulations of the spectra.

DOI: 10.1103/PhysRevA.111.062804

I. INTRODUCTION

Shortly after the discovery of molecular Raman scattering [1], quantum mechanics has been applied to derive formulas explaining observed intensities [2]. In the Placzek approximation the Born-Oppenheimer (BO) concept [3] was used, separating wave functions and energies of the ground and excited vibrational and electronic states. Working equations for polarizabilities that determine Raman intensities were obtained directly from the Schrödinger equation, within Dirac's time-dependent perturbation theory [4,5].

The theory provides so called sum over state (SOS) expressions, direct applications of which did not appear practical. For example, the formulas require knowledge of the excited electronic states, which are hard to get using common quantum-chemical methodologies. In addition, a large number of the states are needed to reproduce the desired polarizabilities.

Instead, derivative-based perturbational methods prevailed, originally restricted to the Hartree-Fock and Møller-Plesset theories [6], later extended within the density functional theory (DFT) [7]. A close inspection of the frequency-dependent electric polarizability provided a way for DFT to be applicable also for excited electronic states, in the form of time-dependent DFT [8]. The derivative approaches are commonly referred to as coupled-perturbed (CP) [9] or response [10] theories. They can be easily extended to simulate polarized Raman spectra and natural vibrational Raman optical activity (ROA) of chiral molecules [5,11–13].

It was also realized that the original formulation of the derivative theory with the time-dependent perturbation approach cannot be used in resonance. In this case, when the Raman excitation frequency matches or is close to the transition energy of an electronic transition, the denominator in the sum over states (SOS) expressions of molecular polarizabilities becomes zero. The computed intensities diverge, and the divergence also affects the CP calculations. As a simple remedy, complex energy formally related to the lifetime of the excited state was introduced [14], which appeared useful also for resonance ROA [15,16]. Depending on the system and experimental conditions, explicit involvement of the vibrational states may be needed as well [17,18].

Below, we address another shortcoming of the derivative approach, the coordinate dependence of energies of the excited electronic states. In the original Placzek approximation gradients of the electronic energies are ignored, whereas common CP expressions contain them. Following this ambiguity, we show that the gradients play a significant role in the modeling of the spectra. A gradient correction of the CP formulas offers a way for alternate, more accurate computations of Raman intensities, particularly important for the resonance phenomena

II. TRANSITION POLARIZABILITIES AND THE PLACZEK APPROXIMATION

Raman intensities are determined by the complex molecular transition polarizability [11,19],

$$\alpha_{\alpha\beta} = \frac{1}{\hbar}\sum_{e\neq i}\frac{\langle f|\mu_\alpha|e\rangle\langle e|\mu_\beta|i\rangle}{\omega_{ei}-\omega-i\Gamma_e} + \frac{1}{\hbar}\sum_{e}\frac{\langle f|\mu_\beta|e\rangle\langle e|\mu_\alpha|i\rangle}{\omega_{ei}+\omega'+i\Gamma_e}, \tag{1}$$

*Contact author: bour@uochb.cas.cz

where i, e, and f denote the initial, intermediate, and final states, respectively, μ_α is an α component of the electric dipole moment operator $\boldsymbol{\mu}$, ω is the excitation frequency, $\omega_{ei} = \omega_e - \omega_i$, ω_e and ω_i are angular frequencies corresponding respectively to the intermediate ("excited") and initial states, ω' is the scattered frequency, and $\hbar$ is the reduced Planck constant. Note that $\omega = \omega' + \omega_f - \omega_i$. The imaginary term $i\Gamma_e$ is proportional to spectral width and accounts for finite lifetime of the state e [11,20].

Similar expressions appear for the four other tensors needed to calculate ROA [21],

$$G_{\alpha\beta} = \frac{1}{\hbar}\sum_{e\neq i,f}\frac{\langle f|\mu_\alpha|e\rangle\langle e|m_\beta|i\rangle}{\omega_{ei}-\omega-i\Gamma_e} + \frac{1}{\hbar}\sum_{e}\frac{\langle f|m_\beta|e\rangle\langle e|\mu_\alpha|i\rangle}{\omega_{ei}+\omega'+i\Gamma_e}, \tag{2a}$$

$$\mathsf{G}_{\alpha\beta} = \frac{1}{\hbar}\sum_{e\neq i,f}\frac{\langle f|m_\alpha|e\rangle\langle e|\mu_\beta|i\rangle}{\omega_{ei}-\omega-i\Gamma_e} + \frac{1}{\hbar}\sum_{e}\frac{\langle f|\mu_\beta|e\rangle\langle e|m_\alpha|i\rangle}{\omega_{ei}+\omega'+i\Gamma_e}, \tag{2b}$$

$$A_{\alpha,\beta\gamma} = \frac{1}{\hbar}\sum_{e\neq i,f}\frac{\langle f|\mu_\alpha|e\rangle\langle e|\Theta_{\beta\gamma}|i\rangle}{\omega_{ei}-\omega-i\Gamma_e} + \frac{1}{\hbar}\sum_{e}\frac{\langle f|\Theta_{\beta\gamma}|e\rangle\langle e|\mu_\alpha|i\rangle}{\omega_{ei}+\omega'+i\Gamma_e}, \tag{2c}$$

$$\mathcal{A}_{\alpha,\beta\gamma} = \frac{1}{\hbar}\sum_{e\neq i,f}\frac{\langle f|\Theta_{\beta\gamma}|e\rangle\langle e|\mu_\alpha|i\rangle}{\omega_{ei}-\omega-i\Gamma_e} + \frac{1}{\hbar}\sum_{e}\frac{\langle f|\mu_\alpha|e\rangle\langle e|\Theta_{\beta\gamma}|i\rangle}{\omega_{ei}+\omega'+i\Gamma_e}, \tag{2d}$$

where $\mathbf{m}$ and $\boldsymbol{\Theta}$ are operators of the magnetic dipole moment and electric quadrupole moment operators, respectively. Since the structure of the ROA tensors is analogous to Eq. (1), their dependence on the gradient will not be discussed separately. However, one has to bear in mind that the magnetic dipole moment is asymmetric, $\langle e|\mathbf{m}|i\rangle = -\langle i|\mathbf{m}|e\rangle$, while $\langle e|\boldsymbol{\mu}|i\rangle = \langle i|\boldsymbol{\mu}|e\rangle$ and $\langle e|\Theta|i\rangle = \langle i|\Theta|e\rangle$. This requires minor modifications of the formulas derived for $\boldsymbol{\alpha}$.

Within the BO formalisms, the wave functions can be written as products of the vibrational (v) and electronic (e) parts, $|i\rangle = |i_e\rangle|i_v\rangle$, etc. Usually, the initial and final electronic states are both equal to the electronic ground state, $|i_e\rangle = |f_e\rangle = |0\rangle$. Following a common computational practice [14,16] we treat the spectral width as a uniform parameter, independent of the states involved, $\Gamma_e = \Gamma\ \forall\ e$. We further define the initial vibrational state $|i_v\rangle = |n\rangle$, intermediate vibrational $|e_v\rangle = |v\rangle$ and electronic $|e_e\rangle = |j\rangle$ states, final vibrational state $|f_v\rangle = |m\rangle$, $\mu_{0j,\alpha} = \langle j|\mu_\alpha|0\rangle$, and $f(\omega_{jv},\omega) = \frac{1}{\omega_{jv}-\omega-i\Gamma} + \frac{1}{\omega_{jv}+\omega'+i\Gamma}$. Then for real wave functions,

$$\alpha_{\alpha\beta} = \frac{1}{\hbar}\sum_{j\neq 0,v}\langle m|\mu_{0j,\alpha}|v\rangle\langle v|\mu_{j0,\beta}|n\rangle f(\omega_{jv},\omega). \tag{3}$$

In the core of the Placzek approach is the treatment of the frequency difference, $\omega_{jv} = \omega_j + \omega_v - \omega_0 - \omega_n$, where the frequencies correspond respectively to excited electronic states j, vibrational states of j, electronic ground state 0, and vibrational states of 0. We can choose the energy scale so that $\omega_0 + \omega_n = 0$ and suppose that the vibrational energies are smaller than the electronic ones, $\omega_v \ll \omega_j$, so that $\omega_{jv} \sim \omega_j$. This makes it possible to sum over the vibrational states, $\sum_v |v\rangle\langle v| = 1$, in Eq. (3). The electronic transition dipole moments $\boldsymbol{\mu}_{oj}$ depend on nuclear coordinates. Taking into account only the linear term, one obtains

$$\alpha_{\alpha\beta} = \frac{1}{\hbar}\sum_{j\neq 0}\langle m|\mu_{0j,\alpha}\mu_{j0,\beta}|n\rangle f(\omega_j,\omega) \approx \sum_{\lambda,\varepsilon}\alpha^{\mathrm{SOS}}_{\lambda\varepsilon,\alpha\beta}\langle m|R^\lambda_\varepsilon|n\rangle, \tag{4}$$

where $\alpha^{\mathrm{SOS}}_{\lambda\varepsilon,\alpha\beta} = \frac{1}{\hbar}\sum_{j\neq 0}\frac{\partial(\mu_{0j,\alpha}\mu_{j0,\beta})}{\partial R^\lambda_\varepsilon}f(\omega_j,\omega)$, and R^λ_ε is a change of the ε coordinate of nucleus λ.

However, Placzek writes [2,5,11,12]

$$\alpha_{\alpha\beta} = \langle m|\alpha_{e,\alpha\beta}(R)|n\rangle \approx \sum_{\lambda,\varepsilon}\alpha^{\mathrm{CP}}_{\lambda\varepsilon,\alpha\beta}\langle m|R^\lambda_\varepsilon|n\rangle, \tag{5}$$

where $\alpha_{e,\alpha\beta} = \frac{1}{\hbar}\sum_{j\neq 0}\mu_{0j,\alpha}\mu_{j0,\beta}f(\omega_j,\omega)$ is the electronic polarizability and $\alpha^{\mathrm{CP}}_{\lambda\varepsilon,\alpha\beta} = \frac{\partial\alpha_{e,\alpha\beta}}{\partial R^\lambda_\varepsilon}$. We use the CP mark to emphasize that this quantity is obtained from the coupled-perturbed computations. Clearly, Eqs. (4) and (5) are not equivalent, as the derivatives of $\boldsymbol{\alpha}_e$ generate an additional gradient (g) term, so that

$$\alpha^{\mathrm{SOS}}_{\lambda\varepsilon,\alpha\beta} = \alpha^{\mathrm{CP}}_{\lambda\varepsilon,\alpha\beta} - \alpha^{g}_{\lambda\varepsilon,\alpha\beta}, \tag{6}$$

with $\alpha^{g}_{\lambda\varepsilon,\alpha\beta} = \frac{1}{\hbar}\sum_{j\neq 0}\mu_{0j,\alpha}\mu_{j0,\beta}g(\omega_j,\omega)(\frac{\partial\omega_j}{\partial R^\lambda_\varepsilon} - \frac{\partial\omega_0}{\partial R^\lambda_\varepsilon})$, where $g(\omega_j,\omega) = -\frac{1}{(\omega_j-\omega-i\Gamma)^2} - \frac{1}{(\omega_j+\omega'+i\Gamma)^2}$.

While the term $\partial\omega_0/\partial R$ proportional to the gradient of the energy in the electronic ground state is often zero as the derivatives are usually evaluated at the equilibrium geometry, zero gradients for the excited states are rarer. The $g(\omega_j,\omega)$ function grows more steeply than $f(\omega_j,\omega)$ when $\omega \to \omega_j$ (Fig. 1), which makes the gradient term particularly important in the resonance and preresonance cases.

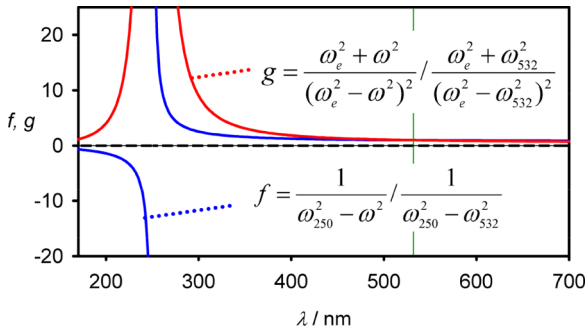

FIG. 1. The g and f functions, for $\Gamma = 0$, relative to their values at 532 nm, for 250 nm transition.

III. ORIGIN DEPENDENCE OF RAMAN OPTICAL ACTIVITY

The approach from above can be readily applied to the ROA polarizabilities. Simulated ROA intensities, however, may depend on the origin of coordinates if approximate wave functions are used. To avoid this, the gauge-independent atomic orbitals (GIAOs) are usually used [22,23], not

applicable within the SOS approach. Instead, we investigate the electronic polarizabilities more closely, introducing a distributed origin gauge (DOG) transformation.

For simplicity, we drop the "e" subscript, and set $\Gamma = 0$ and $\omega = \omega'$, which are frequent practical prerequisites [11]. We also realize that $\mathsf{G}_{e,\alpha\beta} = -G_{e,\beta\alpha}$ and $\mathcal{A}_{e,\alpha,\beta\gamma} = A_{e,\alpha,\beta\gamma}$, so that we are left with three tensors,

$$\alpha_{\alpha\beta} = \frac{2}{\hbar}\sum_{e\neq 0}\frac{\omega_e\langle 0|\mu_\alpha|e\rangle\langle e|\mu_\beta|0\rangle}{\omega_e^2-\omega^2}, \tag{7a}$$

$$G_{\alpha\beta} = \frac{2\omega}{\hbar}\sum_{e\neq 0}\frac{\langle 0|\mu_\alpha|e\rangle\langle e|m_\beta|0\rangle}{\omega_e^2-\omega^2}, \tag{7b}$$

$$A_{\alpha,\beta\gamma} = \frac{2}{\hbar}\sum_{e\neq 0}\frac{\omega_e\langle 0|\mu_\alpha|e\rangle\langle e|\Theta_{\beta\gamma}|0\rangle}{\omega_e^2-\omega^2}. \tag{7c}$$

Let us recall the dipole, magnetic dipole, and quadrupole operators, $\mu_\beta = \sum_i q_i r_{i\beta}$, $m_\beta = \frac{1}{2}\sum_i \frac{q_i}{m_i}\varepsilon_{\beta\gamma\delta} r_{i\gamma} p_{i\delta}$, and $\Theta_{\beta\gamma} = \frac{1}{2}\sum_i q_i(3r_{i\gamma}r_{i\delta} - \delta_{\gamma\delta}r_i^2)$ [5,11], since alternate definitions exist in literature. We use the GAUSSIAN program [24] that calculates the quadrupole elements using a mixed length-velocity formalism, exploring the identity $\langle e|r_\alpha r_\beta|0\rangle = \frac{-\hbar}{m_e\omega_{e0}}\langle e|r_\alpha\nabla_\beta + r_\beta\nabla_\alpha|0\rangle$. Let us shift the coordinates by $\mathbf{T}$. Then $\boldsymbol{\alpha}$ is not changed, whereas the other two tensors become

$$G_{\alpha\beta}(\mathbf{T}) = G_{\alpha\beta}(0) + \frac{i\omega}{2}\varepsilon_{\beta\gamma\delta}T_\gamma\alpha^v_{\alpha\delta}, \tag{8a}$$

$$A_{\alpha,\beta\gamma}(\mathbf{T}) = A_{\alpha,\beta\gamma}(0) + \frac{3}{2}\left(T_\gamma\alpha^v_{\alpha\beta} + T_\beta\alpha^v_{\alpha\gamma}\right) - \delta_{\beta\gamma}T_\varepsilon\alpha^v_{\alpha\varepsilon}, \tag{8b}$$

where the velocity form of $\boldsymbol{\alpha}$ is $\alpha^v_{\alpha\delta} = 2\sum_{e\neq 0}\frac{\langle 0|\mu_\alpha|e\rangle\langle 0|\sum_i\frac{q_i}{m_i}\nabla_{i\delta}|e\rangle}{\omega_e^2-\omega^2}$. In Eqs. (8a) and (8b) "(0)" indicates the values before the shift. Using the dipole-velocity transformation, $\langle 0|p_\delta|e\rangle = -i\omega_{e0}m\langle e|r_\delta|0\rangle$, we obtain $\alpha^v_{\alpha\delta} = \alpha_{\alpha\delta}$, but this is not generally true for approximate wave functions. For example, while $\alpha_{\alpha\delta} = \alpha_{\delta\alpha}$, $\alpha^v_{\alpha\delta}$ is not symmetric.

ROA intensity of isotropic samples depends on tensor invariants. For commonly used backscattering and scattered circular polarization (SCP), it is proportional to [5]

$$I_{\mathrm{ROA}} = k(3\alpha_{\alpha\beta}G_{\beta\alpha} - \alpha_{\alpha\alpha}G_{\beta\beta} + \varepsilon_{\alpha\beta\gamma}\alpha_{\alpha\delta}A_{\beta,\gamma\delta}), \tag{9}$$

where k is a constant; for brevity we do not indicate a particular transition or derivative, and use the Einstein summation convention. When the velocity form $\boldsymbol{\alpha}^v$ is used, the first and last terms in Eq. (9) are origin independent since the extra terms arising due to the shift vanish [$\alpha^v_{\alpha\beta}\varepsilon_{\beta\gamma\delta}T_\gamma\alpha^v_{\alpha\delta} = 0$ and $\varepsilon_{\alpha\beta\gamma}\alpha^v_{\alpha\delta}(\frac{3}{2}(T_\delta\alpha^v_{\beta\gamma} + T_\gamma\alpha^v_{\beta\delta}) - \delta_{\gamma\delta}T_\varepsilon\alpha^v_{\beta\varepsilon}) = 0$]. The second term is origin independent only with the symmetric $\boldsymbol{\alpha}$, when $\varepsilon_{\beta\gamma\delta}T_\gamma\alpha_{\beta\delta} = 0$.

To minimize the origin dependence, we transform polarizability derivatives computed in the common origin gauge (COM) to a distributed origin gauge (DOG), and use them in Eq. (9). For derivatives with respect to nucleus λ and coordinate ε,

$$G_{\lambda\varepsilon,\alpha\beta}(\mathrm{DOG}) = G_{\lambda\varepsilon,\alpha\beta}(\mathrm{COM}) + \frac{i\omega}{2}\varepsilon_{\beta\varepsilon\delta}R^\lambda_\varepsilon\Delta\alpha_{\lambda\varepsilon,\alpha\delta}, \tag{10a}$$

$$A_{\lambda\varepsilon,\alpha,\beta\gamma}(\mathrm{DOG}) = A_{\lambda\varepsilon,\alpha,\beta\gamma}(\mathrm{COM}) + \frac{3}{2}\left(R^\lambda_\beta\Delta\alpha_{\lambda\varepsilon,\alpha\gamma} + R^\lambda_\gamma\Delta\alpha_{\lambda\varepsilon,\alpha\beta}\right) - \delta_{\beta\gamma}R^\lambda_\varepsilon\Delta\alpha_{\lambda\varepsilon,\alpha\varepsilon}, \tag{10b}$$

where $\Delta\alpha_{\lambda\varepsilon,\alpha\delta} = \alpha_{\lambda\varepsilon,\alpha\delta} - \alpha^v_{\lambda\varepsilon,\alpha\delta}$. After a coordinate shift $\mathbf{T}$ the tensors change to

$$G_{\lambda\varepsilon,\alpha\beta}(\mathrm{DOG},T) = G_{\lambda\varepsilon,\alpha\beta}(\mathrm{DOG},0) + \frac{i\omega}{2}\varepsilon_{\beta\varepsilon\delta}T_\varepsilon\alpha_{\lambda\varepsilon,\alpha\delta}, \tag{11a}$$

$$A_{\lambda\varepsilon,\alpha,\beta\gamma}(\mathrm{DOG},T) = A_{\lambda\varepsilon,\alpha,\beta\gamma}(\mathrm{DOG},0) + \frac{3}{2}(T_\beta\alpha_{\lambda\varepsilon,\alpha\gamma} + T_\gamma\alpha_{\lambda\varepsilon,\alpha\beta}) - \delta_{\beta\gamma}T_\varepsilon\alpha_{\lambda\varepsilon,\alpha\varepsilon}. \tag{11b}$$

For applied computations, one has to realize that the GAUSSIAN program computes derivatives of transition gradients, not of the transition dipole moment in the velocity representation. The latter needed for $\boldsymbol{\alpha}^v$ can be obtained from the former as $\frac{\partial 0|\mu^v_\delta|e}{\partial R^\lambda_\varepsilon} = \frac{\hbar}{\omega_{e0}}\frac{\partial 0|\sum_i\frac{q_i}{m_i}\nabla_{i\delta}|e}{\partial R^\lambda_\varepsilon}$. The dependence on ω_{e0} requires that one uses the different gradient parts of $\boldsymbol{\alpha}^v$ for $\mathbf{G}$ and $\mathbf{A}$. Specifically, we use

$$\alpha^{vg}_{\lambda\varepsilon,\alpha\delta} = \sum_{e\neq 0}\langle 0|\mu_\alpha|e\rangle\langle 0|\mu^v_\delta|e\rangle\left[\frac{1}{(\omega_e-\omega)^2} - \frac{1}{(\omega_e+\omega)^2}\right]\frac{\omega_e}{\omega} \times\left(\frac{\partial\omega_e}{\partial R^\lambda_\varepsilon} - \frac{\partial\omega_0}{\partial R^\lambda_\varepsilon}\right)$$

in Eq. (10a) and

$$\alpha^{vg}_{\lambda\varepsilon,\alpha\delta} = \sum_{e\neq 0}\langle 0|\mu_\alpha|e\rangle\langle 0|\mu^v_\delta|e\rangle\left[\frac{1}{(\omega_e-\omega)^2} + \frac{1}{(\omega_e+\omega)^2}\right] \times\left(\frac{\partial\omega_e}{\partial R^\lambda_\varepsilon} - \frac{\partial\omega_0}{\partial R^\lambda_\varepsilon}\right)$$

in Eq. (10b).

IV. IMPLEMENTATION

To investigate the impact of the gradient terms, we corrected CP polarizabilities using Eq. (6). Alternatively, one could also consider the possibility to calculate $\boldsymbol{\alpha}^{\mathrm{SOS}}$ directly using Eq. (4). There are, however, three serious obstacles for this way. First, the SOS computational scheme is notoriously slow and computationally demanding [25]. Second, the dipole derivatives needed in Eq. (4) are ill defined for degenerate states (cf. below). Finally, plain SOS ROA intensities would suffer from the origin dependence [5,26]. Using formula (6) instead of (4) has also the advantage that only some of the excited states need to be calculated, since the lowest-energy ones contribute most.

For the first model system, we chose hydrogen peroxide (H_2O_2), where all the excited electronic states within time-dependent DFT (TDDFT) can be comfortably computed. Their number is approximately the number of occupied orbitals times the number of virtual orbitals [27]. "Real-life" molecules include α-pinene and camphor as typical far from resonance systems serving for calibration of

the Raman and ROA techniques [28–30], and (*S*,*S*)-N,N-ethylenediaminedisuccinic iron and cobalt complexes (Fe^{III} EDDS, Co^{III} EDDS), where the preresonance effects can be demonstrated. Experimental Co^{III} EDDS Raman and ROA spectra were reported lately [17]; chemical synthesis and measurement details for Fe^{III} EDDS are described in the Supplemental Material [31]. The spectra were measured on a Zebr spectrometer [34] operating in a backscattering scattered circular polarization (SCP) mode and using 532-nm laser excitation. α-pinene was used as neat liquid, camphor was measured as a solution in methanol, and water solutions of the complexes were used.

The GAUSSIAN program [24] was used to compute equilibrium geometries, harmonic molecular force fields, CP polarizability derivatives, excited electronic states, transition electric/magnetic dipoles and quadrupoles, their derivatives, and gradients of the ground and excited state energies, applying the common B3LYP [35] functional, standard 6-311++G** basis set, and CPCM [36,37] solvent model with parameters for toluene (for α-pinene), methanol (camphor), and water (the complexes). For the complexes, the geometry and harmonic force field were calculated with the double-hybrid PBEQIDH [38] functional instead, as B3LYP was found slightly less accurate [17]. The SOS expressions for the tensor derivatives were computed using ours scripts ("Polderdip" and minor programs), including 800, 400, and 200 electronic excited states for α-pinene, camphor, and EDDS complexes, respectively. Convergence tests suggest that they recover most of the gradient correction [31].

Raman and ROA intensities for each normal mode i were obtained from the polarizability derivatives as [5,11]

$$I_{\mathrm{Raman}} = K \sum_{\alpha=1}^{3}\sum_{\beta=1}^{3}\left(\alpha^i_{\alpha\alpha}\alpha^i_{\beta\beta} + 7\alpha^i_{\alpha\beta}\alpha^i_{\alpha\beta}\right), \tag{12}$$

$$I_{\mathrm{ROA}} = 8K \sum_{\beta=1}^{3}\sum_{\alpha=1}^{3}\left(3\alpha^i_{\alpha\beta}G'^i_{\alpha\beta} - \alpha^i_{\alpha\alpha}G'^i_{\beta\beta} + \sum_{\varepsilon=1}^{3}\sum_{\gamma=1}^{3}\varepsilon_{\alpha\beta\gamma}\alpha^i_{\alpha\varepsilon}A^i_{\beta\gamma\varepsilon}\right), \tag{13}$$

where $\mathbf{G}' = -\mathrm{Im}(\mathbf{G})$, K is a constant, and the subscript i denotes derivatives with respect to this normal mode coordinate. These were obtained, for example, as $\alpha^i_{\alpha\beta} = \sum_\lambda \sum_\varepsilon \alpha_{\lambda\varepsilon,\alpha\beta} S_{i,\lambda\varepsilon}$, where $\mathbf{S}$ is the Cartesian-normal mode transformation matrix. Smooth spectra were generated from the intensities as

$$S(\omega) = \sum_i I_i\left[1 - \exp\left(-\frac{\omega_i}{kT}\right)\right]^{-1}\left[4\left(\frac{\omega-\omega_i}{\Delta}\right)^2 + 1\right]^{-1}, \tag{14}$$

where ω_i is the vibrational frequency, k is the Boltzmann constant, T is the temperature, and $\Delta = 10\ \mathrm{cm}^{-1}$. For comparison with the experiment, calculated spectra were normalized to integrated experimental Raman areas.

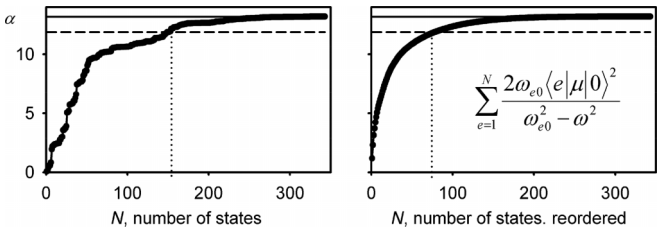

FIG. 2. Calculated (for H_2O_2, B3LYP/6-311++G**, $\lambda = 250$ nm, $\Gamma = 0$) isotropic polarizability as dependent on the number of states ordered by their energy (left) and contribution (right). The solid line marks the exact CP value. The dashed line marks 90%, and achieved for 149 states on the left and 78 states after the reordering.

V. RESULTS AND DISCUSSION

A. SOS convergence, gradient parts of the derivatives

For H_2O_2, convergence and other properties of the polarizabilities calculated by the SOS method can be conveniently demonstrated. With the 6-311++G** basis set the TDDFT method generates in total 343 electronic excited states. The dependence of the isotropic polarizability on the number of states taken is plotted in Fig. 2. The convergence is relatively slow, which corresponds to previous experience [25,39]. If the states are ordered according to their energy (left in the figure), 149 states recover 90% of the polarizability. When they are ordered according to their contributions to the polarizability, only 78 states are needed for the same result. Of course, to order them all states need to be calculated anyway. However, we point out the possibility of the preselection to potentially speed up computations of the polarizability derivatives. The SOS computation with all states included fully recovers the CP value, which shows that within TDDFT the CP and SOS methods are equivalent.

In Fig. 3 the convergence is investigated also for the G and A tensors, and the derivatives of α, G, and A. Interestingly, the isotropic part of G converges faster those of α and A; in addition, its convergence is not monotonic since the $G_{\alpha\alpha}$ elements can be both positive and negative. The derivatives converge faster than the tensors themselves, however, the dependencies are not smooth, with jumps caused by singularities stemming from the degenerate states. For molecules larger than the peroxide these instabilities practically prevent direct SOS computations of the tensor derivatives. On the other hand, the gradient parts of the tensors (red in the figure) do not suffer from these singularities, and converge smoothly and quickly. Interestingly, for the G tensor the gradient part is larger than the total. However, note that the invariant is not a simple sum of the gradient and the SOS parts.

The relative contributions of the SOS and gradient parts of H_2O_2 α-derivative elements calculated for two excitation wavelengths are plotted in Fig. 4. The gradient part is very significant for the 250-nm excitation, close to the lowest-energy electronic transition at 224 nm. The gradient part often dominates; outstanding is the fourth element where the dipole derivative part is negative. The gradient parts are on average smaller for the 532-nm excitation, although they occasionally contribute by more than 50% also here.

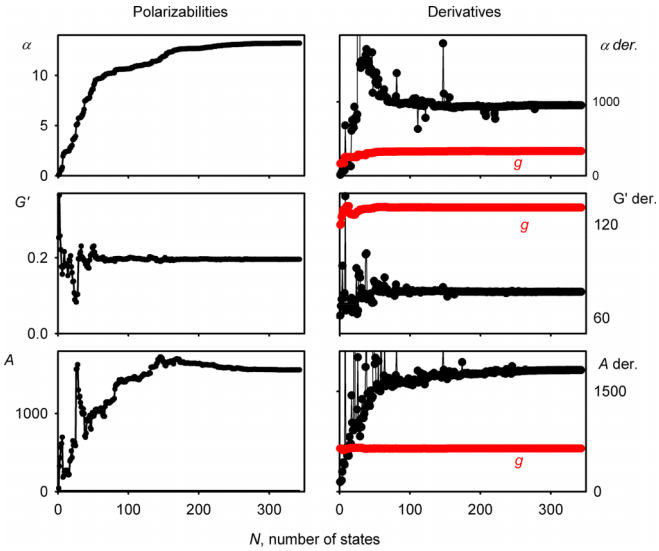

FIG. 3. H_2O_2, calculated dependencies of the polarizability [left; $\alpha_{\alpha\alpha}$, $G_{\alpha\alpha}$, $2A_{\alpha,\alpha\beta}$ $(A_{\beta,\gamma\gamma}+2A_{\gamma,\beta\gamma})$ + $A_{\alpha,\beta\beta}$ $(A_{\alpha,\gamma\gamma}+2A_{\gamma,\alpha\gamma})$ + $2A_{\alpha,\beta\gamma}$ $(A_{\alpha,\beta\gamma}+A_{\beta,\alpha\gamma}+A_{\gamma,\alpha\beta})$] and polarizability derivative (right; $\sum_{\varepsilon,\lambda,\alpha}\alpha^2_{\lambda\varepsilon,\alpha\alpha}$, $\sum_{\varepsilon,\lambda,\alpha}G^2_{\lambda\varepsilon,\alpha\alpha}$, $\sum_{\varepsilon,\lambda,\alpha}A^2_{\lambda\varepsilon,\alpha\alpha\alpha}$) invariants on the number of the electronic states. Gradient parts of the derivatives are plotted in red.

B. Degeneracy problem in computations of the transition moments

To better understand the singularities observed for the tensor derivatives in Fig. 3, let us consider a simplified system with only two (nearly) degenerate excited electronic states A and B. These are eigenfunctions of a Hamiltonian H, $H|A\rangle = \omega_A|A\rangle$ and $H|B\rangle = \omega_B|B\rangle$. In their contributions to the polarizability we neglect the nonresonance parts, do not explicitly write the indices, and set $\hbar = 1$, so that

$$\alpha = \frac{\langle 0|\mu|A\rangle\langle A|\mu|0\rangle}{\omega_A - \omega} + \frac{\langle 0|\mu|B\rangle\langle B|\mu|0\rangle}{\omega_B - \omega}. \tag{15}$$

Setting $\omega_A \sim \omega_B \sim \bar{\omega}$ and abbreviating $\mu_A = \langle 0|\mu|A\rangle$, this becomes $\alpha = (\mu_A^2 + \mu_B^2)/(\bar{\omega} - \omega)$.

A derivative can be though of as a limit, for example

$$\frac{\partial \mu_A}{\partial x} = \lim_{d\to 0}\frac{\mu_A(x_0+d) - \mu_A(x_0)}{d}, \tag{16}$$

where x_0 is the equilibrium geometry. After the $x_0 \to x_0 + d$ geometry change the Hamiltonian changes to $H + V$ and new

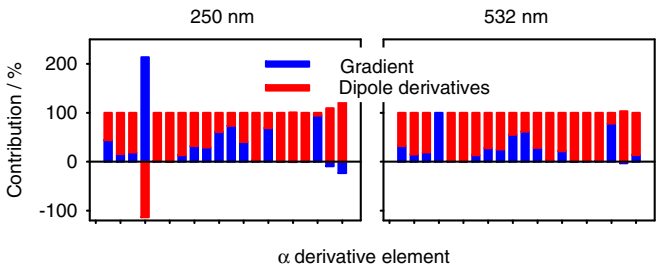

FIG. 4. H_2O_2, relative contributions of the SOS and gradient parts to α-derivative elements at 250- and 532-nm excitations, B3LYP/6–311++G** calculation.

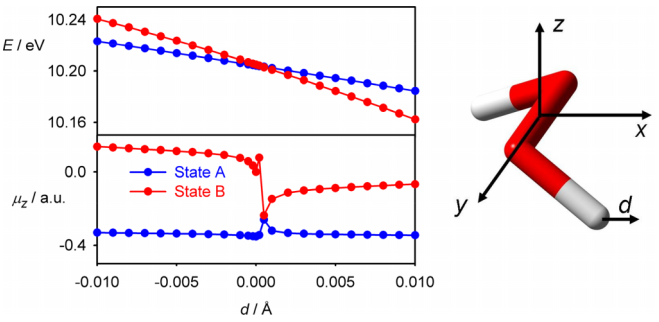

FIG. 5. Calculated dependence (B3LYP/6-311++G**) of energies and dipole moments of degenerate transitions (number 8 and 9) of H_2O_2 on the deviation of a hydrogen from its equilibrium position. We can see a singularity at the equilibrium geometry, preventing reliable estimation of the transition dipole moment derivatives.

states can be approximately considered as a mix of A and B, obeying the Schrödinger equation,

$$(H+V)(c_A|A\rangle + c_B|B\rangle) = \omega'(c_A|A\rangle + c_B|B\rangle), \tag{17}$$

which can be written in a matrix form,

$$\begin{pmatrix} \bar{\omega}-\omega' & v \\ v & \bar{\omega}-\omega' \end{pmatrix}\begin{pmatrix} c_A \\ c_B \end{pmatrix} = 0, \tag{18}$$

where $v = \langle A|V|B\rangle = \langle B|V|A\rangle$ and we supposed that $\langle A|V|A\rangle \ll \bar{\omega}$ and $\langle B|V|B\rangle \ll \bar{\omega}$. The new energies, wave functions, and transition dipole moments are respectively $\omega'_\pm = \omega \pm |v|$, $|\pm\rangle = (|A\rangle \pm |B\rangle)/\sqrt{2}$, and $\mu_A(x_0+d) = [\mu_A(x_0) + \mu_B(x_0)]/\sqrt{2}$. However, now the derivative in Eq. (16) is ill-defined since it becomes

$$\frac{\partial \mu_A}{\partial x} = \lim_{d\to 0}\frac{[\mu_A(x_0)+\mu_B(x_0)]/\sqrt{2} - \mu_A(x_0)}{d} \to \pm\infty. \tag{19}$$

This is a general problem; for example, we observed similar difficulties in differentiations with degenerate wave functions in Ref. [40]. An example of actual dependence of the transition dipole moments in H_2O_2 on a nuclear coordinate as calculated by the GAUSSIAN program [24] is in Fig. 5.

C. Gradient-corrected Raman and ROA spectra

Although the direct computation of the polarizability derivatives using the SOS formulas is hindered by the degeneracies and other problems, the correction of the CP results for the gradient part appears viable. For the larger molecules, we can see the effects of the gradient term on Raman and ROA spectra of α-pinene, camphor, and the complex in Fig. 6. The CP results are compared to those when the gradient part was subtracted [Eq. (6)], and to the experiment.

For α-pinene and camphor, the differences caused by the gradient are rather minor; the most apparent one is the large (∼80%) drop of the Raman intensity of the C = C stretching band of α-pinene (∼1657 cm^{-1}). Experimentally, this band is weaker than the neighboring 1437-cm^{-1} CH_3 umbrella band, so the correction goes to the right direction, but is too big. A clearer improvement is achieved in the CH bending region of ∼1200–1350 cm^{-1}. In the figure we marked some bands where the gradient subtraction was profitable by green stars,

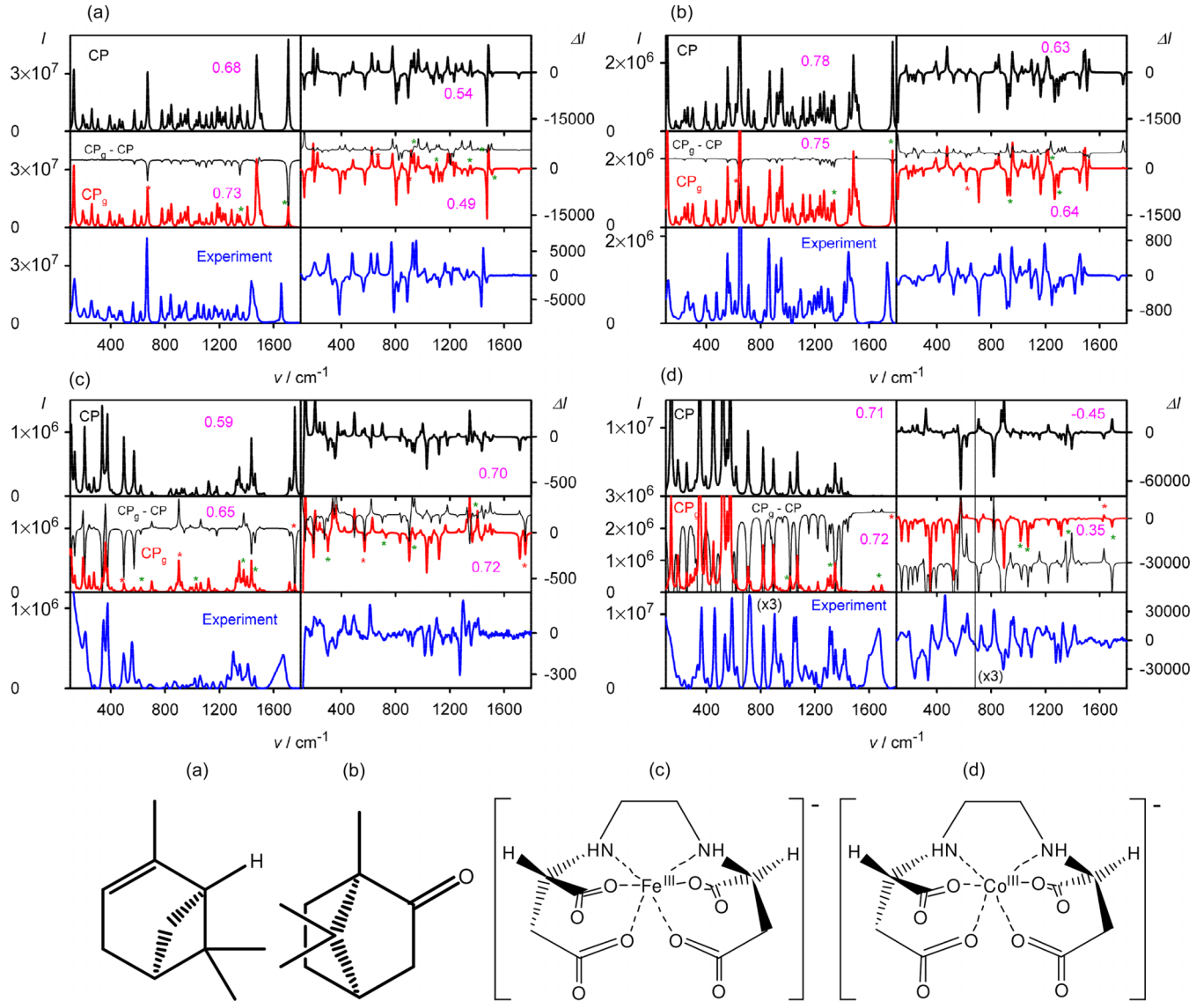

FIG. 6. Raman and ROA spectra of (a) (1*S*)-(-)-α-pinene, (b) (1*R*)-(+)-camphor, (c),(d) (*S*,*S*)-N,N-ethylenediaminedisuccinic iron/cobalt complexes (Fe^{III} EDDS/Co^{III} EDDS), calculated by the plain coupled perturbed B3LYP/6-311++G**/CPCM calculation (CP, thick black), with polarizability tensors where the gradient part was subtracted (CP_g, red, CP_g-CP, thin black, is the difference spectrum), and experiment (blue). The magenta spectra numbers indicate similarities ($s = \int S_{cal} S_{exp} d\nu / \sqrt{\int S_{cal}^2 d\nu \int S_{exp}^2 d\nu}$) to the experiment, red (green) stars indicate examples of relative intensity deteriorations (improvements) of CP_g against CP; 532 nm excitation was used in the calculations and the experiment.

while a red star indicates a worse result compared to the experiment. As another criterion, the similarity indices (s) are indicated, too. In terms of the similarities, the gradient subtraction improved the calculated Raman spectra of α-pinene (0.68 → 0.73) and made worse those of camphor (0.78 → 0.75).

For ROA spectra, the effect of the gradient subtraction on the relative intensities is bigger than for Raman. Especially above 1000 cm^{-1}, there are many bands profiting from it, although on average the "corrected" spectrum seems to be worse for α-pinene (0.54 → 0.49) and only slightly better (0.63 → 0.64) for camphor.

The energies of the electronic transitions in the Fe^{III} EDDS complex are much closer to the excitation laser line (cf. the UV spectra in the Supplemental Material [31]), which makes the effect of the gradient subtraction much more significant. Compared to the pure CP spectrum, the "CP_g" Raman pattern is much improved, especially within 1200–1500 cm^{-1}, and the similarity rises (0.59 → 0.65). One has to admit that compared to α-pinene and camphor, neither the CP nor CP_g give a particularly satisfactory representation to the experiment. Analysis of the reasons goes beyond the scope of the present study as it may be related to the high multiplicity ($M = 6$) of the complex, internal DFT error, approximate solvent model, and many resonance or preresonance phenomena [17].

For ROA large differences between the CP and CP_g intensities are apparent as well; some ROA bands even change sign after the gradient subtraction. Quite often, the gradient

correction goes to the desired trend, such as giving the right ROA sign, but the final intensity is too large or weak, i.e., the correction is "overdone." A minor improvement in terms of overall similarity to experiment (0.70 → 0.72) is thus achieved.

Finally, for the Co EDDS complex, the largest effects of the gradient correction are observed. The correction leads to negligible statistical improvement (similarity increase 0.71 → 0.72) for Raman, although the relative intensities of many bands are becoming more realistic. For ROA, however, the similarity increases significantly (−0.54 → 0.35), and the simulated spectrum becomes more realistic, in particular above 800 cm^{-1}. For low wave numbers, explicit consideration of vibrational states may be needed, as discussed in Ref. [17].

Overall, we can see that the correction is extremely important to consider in resonance; however, band-to-band reproduction of Raman and ROA spectra in this case becomes extremely challenging. The gradient issue thus appears as one of many aspects in the process of developing suitable computational methodology.

Technically, the correction itself [Eq. (6)] can be realized relatively easily as analytical computations of excited state gradients [41] have been implemented in common quantum chemical software [24,42]. The possibility to compute the gradients is already explored in many other contexts of Raman [43] and one-electron [44] spectroscopies.

VI. CONCLUSIONS

We have found that the dependence of the electronic energies on nuclear coordinates neglected in the Placzek's and CP approaches has a considerable effect on the Raman and Raman optical activity intensities. Significant intensity variations could be observed already for the far from resonance cases, and proper treatment of the gradients seem to be of even greater significance in the resonance Raman spectroscopy. For Raman optical activity, we developed a distribute-origin transformation enabling one to avoid the origin dependence of the results. The data show that the gradient part cannot be ignored in precise computation of the intensities. It can be relatively easily computed, and converges smoothly with the number of electronic states included. It becomes particularly important in the dynamically evolving fields of resonance Raman scattering, plasmonic, and surface-enhanced phenomena.

ACKNOWLEDGMENT

The work was supported by the Grant Agency of the Czech Republic (Grant No. 25-15726S).

DATA AVAILABILITY

The data that support the findings of this article are included in the text and in the Supplemental Material.

[1] C. V. Raman, Indian J. Phys. **2**, 387 (1928).
[2] G. Placzek, in *Handbuch der Radiologie*, edited by E. Marx (Akademische Verlagsgesellschaft, Leipzig, 1934), pp. 209–374.
[3] M. Born and R. Oppenheimer, Ann. Phys. **84**, 457 (1927).
[4] P. A. M. Dirac, *The Principles of Quantum Mechanics* (Cambridge University Press, Cambridge, UK, 1930).
[5] L. D. Barron, *Molecular Light Scattering and Optical Activity* (Cambridge University Press, Cambridge, UK, 2004).
[6] J. A. Pople, R. Krishnan, H. B. Schlegel, and J. S. Binkley, Int. J. Quantum Chem. **16**, 225 (1979).
[7] S. J. A. van Gisbergen, J. G. Snijders, and E. J. Baerends, Chem. Phys. Lett. **259**, 599 (1996).
[8] J. Guan, P. Duffy, J. T. Carter, D. P. Chong, K. C. Casida, M. E. Casida, and M. Wrinn, J. Chem. Phys. **98**, 4753 (1993).
[9] A. G. Ioannou and R. D. Amos, Chem. Phys. Lett. **279**, 17 (1997).
[10] P. Norman, K. Ruud, and T. Saue, *Principles and Practices of Molecular Properties* (Wiley, Oxford, 2018).
[11] L. Nafie, *Vibrational Optical Activity: Principles and Applications* (Wiley, Chichester, 2011).
[12] V. Liegeois, K. Ruud, and B. Champagne, J. Chem. Phys. **127**, 204105 (2007).
[13] T. Wu, G. Li, J. Kapitán, J. Kessler, Y. Xu, and P. Bouř, Angew. Chem. Int. Ed. **59**, 21895 (2020).
[14] L. Jensen, L. L. Zhao, J. Autschbach, and G. C. Schatz, J. Chem. Phys. **123**, 174110 (2005).
[15] G. Zając and P. Bouř, J. Phys. Chem. B **126**, 355 (2022).
[16] G. Li, M. Alshalalfeh, W. Yang, J. R. Cheeseman, P. Bouř, and Y. Xu, Angew. Chem. Int. Ed. **60**, 22004 (2021).
[17] Q. Yang, J. Bloino, H. Šestáková, J. Šebestík, J. Kessler, J. Hudecová, J. Kapitán, and P. Bouř, Angew. Chem. Int. Ed. **62**, e202312521 (2023).
[18] A. Baiardi, J. Bloino, and V. Barone, J. Chem. Theory Comput. **14**, 6370 (2018).
[19] R. Dick, in *Advanced Quantum Mechanics*, edited by R. Dick (Springer, Cham, 2020).
[20] L. Nafie, Theor. Chem. Acc. **119**, 39 (2008).
[21] L. Hecht and L. A. Nafie, Mol. Phys. **72**, 441 (1991).
[22] T. Helgaker, K. Ruud, K. L. Bak, P. Joergensen, and J. Olsen, Farad. Discuss. **99**, 165 (1994).
[23] J. R. Cheeseman and M. J. Frisch, J. Chem. Theory Comput. **7**, 3323 (2011).
[24] M. J. Frisch *et al.*, *GAUSSIAN 16 Rev. A.03* (Gaussian, Inc., Wallingford, CT, 2016).
[25] J. P. Coe and M. J. Paterson, J. Chem. Phys. **141**, 124118 (2014).
[26] P. Bouř, J. Comput. Chem. **22**, 426 (2001).
[27] F. Furche and R. Ahlrichs, J. Chem. Phys. **117**, 7433 (2002).
[28] P. Bouř, J. McCann, and H. Wieser, J. Phys. Chem. A **102**, 102 (1998).
[29] P. Bouř, V. Baumruk, and J. Hanzlíková, Collect. Czech. Chem. Commun. **62**, 1384 (1997).
[30] J. Hudecová, V. Profant, P. Novotná, V. Baumruk, M. Urbanová, and P. Bouř, J. Chem. Theory Comput. **9**, 3096 (2013).
[31] See Supplemental Material at http://link.aps.org/supplemental/10.1103/PhysRevA.111.062804 for synthesis and UV spectra of [FeEDDS]NH_4, and dependence of the gradient part in calculated α-pinene spectra on the number of states. The Supplemental Material also contains Refs. [32] and [33].

[32] J. A. Neal and N. J. Rose, Inorg. Chem. **7**, 2405 (1968).
[33] N. P. Chmel, S. E. Howson, L. E. N. Allan, J. Barker, G. J. Clarkson, S. S. Turner, and P. Scott, Dalton Trans. **39**, 2919 (2010).
[34] P. Michal, R. Čelechovský, M. Dudka, J. Kapitán, M. Vůjtek, M. Berešová, J. Šebestík, K. Thangavel, and P. Bouř, J. Phys. Chem. B **123**, 2147 (2019).
[35] A. D. Becke, J. Chem. Phys. **98**, 5648 (1993).
[36] M. Cossi, N. Rega, G. Scalmani, and V. Barone, J. Comput. Chem. **24**, 669 (2003).
[37] A. Klamt, in *The Encyclopedia of Computational Chemistry*, edited by P. R. Schleyer, N. L. Allinger, P. A. Kollman, T. Clark, and H. F. Schaefer III (John Wiley & Sons, Chichester, 1998), pp. 604–615.
[38] E. Brémond, J. C. Sancho-García, A. J. Pérez-Jiménez, and C. Adamo, J. Chem. Phys. **141**, 031101 (2014).
[39] P. Bouř, Chem. Phys. Lett. **265**, 65 (1997).
[40] J. Tomeček and P. Bouř, J. Chem. Theory Comput. **16**, 2627 (2020).
[41] G. Scalmani, M. J. Frisch, B. Mennucci, J. Tomasi, R. Cammi, and V. Barone, J. Chem. Phys. **124**, 094107 (2006).
[42] G. te Velde, F. M. Bickelhaupt, E. J. Baerends, C. Fonseca Guerra, S. J. A. van Gisbergen, J. G. Snijders, and T. Ziegler, J. Comput. Chem. **22**, 931 (2001).
[43] F. Zutterman, V. Liégeois, and B. Champagne, J. Phys. Chem. B **126**, 3414 (2022).
[44] D. Padula, D. Picconi, A. Lami, G. Pescitelli, and F. Santoro, J. Phys. Chem. A **117**, 3355 (2013).